DOI: 10.1002/ejic.200900791

Structure and Properties of Copper(II), Manganese(III), and Iron(III) Complexes with Potentially Pentaanionic Heptadentate Ligands Including Alkoxido, Amido, and Phenoxido Donors

Liliana Stoicescu,*[a] Carine Duhayon,[b] Laure Vendier,[b] Ana Tesouro-Vallina,[b] Jean-Pierre Costes,[b] and Jean-Pierre Tuchagues*[b]

Keywords: Dinuclear complexes / Coordination modes / Copper / Iron / Manganese / Magnetic properties

The synthesis and characterization of copper(II), manganese(III), and iron(III) complexes $[Cu_2(L^1)(OAc)Cs_2(MeOH)_2]_n$ (**1**), $[Mn_2(H_3L^1)_2(OMe)_2]\cdot 2MeOH$ (**2**), $[Fe_2(H_3L^1)_2(Hpz)_4](ClO_4)_2\cdot 2CH_3CN$ (**3**), and $[Fe_2(H_3L^3)_2(OMe)_2]\cdot 8MeOH$ (**4**) of potentially pentaanionic heptadentate ligands, 2-hydroxy-*N*-{2-hydroxy-3-[(2-hydroxybenzoyl)amino]propyl}benzamide (H_5L^1) and 2-hydroxy-*N*-{3-hydroxy-5-[(2-hydroxybenzoyl)amino]pentyl}benzamide (H_5L^3), are reported. The crystal structure and magnetic properties of these complexes have been determined. In complex **1**, the ligand H_5L^1 acts as a heptadentate, fully deprotonated ligand, $[L^1]^{5-}$. In complexes **2**, **3**, and **4**, H_5L^1 (**2**, **3**) and H_5L^3 (**4**) act as tetradentate, partially deprotonated ligands, $[H_3L^1]^{2-}$ and $[H_3L^3]^{2-}$. In complex **1**, anionic $[Cu_2(L^1)(OAc)]^{2-}$ and cationic $[Cs(MeOH)]^+$ units are linked through a quadruply bridging acetate ion and through the phenoxido-oxygen and amido-oxygen donor atoms of $[L^1]^{5-}$ to yield a 2D polymeric network. Complexes **2**–**4** form extended supramolecular networks. Magnetic susceptibility data evidence antiferromagnetic interactions for **1**, **2**, and **4**. The Fe···Fe distance is too long to allow measurable magnetic interactions in complex **3**.

Introduction

Transition-metal complexes with ligands containing one,[1–10] two,[11–41] or three[42–46] 2-hydroxybenzamido moieties have been the subject of many reports. Attention has been focused on the copper(II),[11–16] nickel(II),[13,16,17] cobalt(II),[18] cobalt(III),[19–21] cobalt(IV),[22] iron(II),[23–25] iron(III),[23,25–28] manganese(III),[29–32] manganese(IV),[33] chromium(III),[26,34] oxovanadium(IV),[35,36] oxovanadium(V),[36] ruthenium(IV),[37] nitridoruthenium(VI),[38] osmium(III),[39] osmium(IV),[40,41] and nitridoosmium(VI)[38] complexes with ligands containing two 2-hydroxybenzamido moieties. Some of these metal complexes exhibit interesting redox, catalytic, spectral, and magnetic properties.

The bis(2-hydroxybenzamides) are polyanionic, polydentate ligands and have proved to be excellent candidates for stabilizing the higher oxidation states of transition metals. The most studied ligands of this type have been the potentially tetraanionic hexa-, hepta-, octa-, and nonadentate ligands. Very little information has been published on the transition-metal complexes with potentially pentaanionic ligands incorporating two 2-hydroxybenzamido moieties. From the potentially dinucleating, pentaanionic, heptadentate ligand that include alkoxido, amido, and phenoxido donors, Bertoncello et al.[32] have obtained doubly bridged μ-alkoxido-μ-acetato manganese(III) complexes with the general formula $[Mn_2(L^1)(OAc)(B)_4]$ (B = pyridine, γ-picoline and methanol, H_5L^1 = 2-hydroxy-*N*-{2-hydroxy-3-[(2-hydroxybenzoyl)amino]propyl}benzamide).

Chowdhury et al.[27] have obtained the dinuclear Fe^{III}–Fe^{III} and Fe^{III}–Zn^{II} complexes of a potentially dinucleating, pentaanionic, nonadentate ligand that incorporate two 2-hydroxybenzamide moieties and an imidazoline backbone. In a recent paper,[30] we described the crystal structures and properties of doubly bridged, μ-alkoxido-μ-X (X = pyrazolato or acetato) dinuclear manganese(III) complexes $[Mn_2(L^1)(OAc)(MeOH)_4]$, $[Mn_2(L^1)(pz)(MeOH)_4]\cdot 0.5MeOH$, and $[Mn_2(L^2)(pz)(MeOH)_4]$ (AcOH = acetic acid, Hpz = pyrazole) with the potentially dinucleating, pentaanionic, heptadentate ligands including alkoxido, amido, and phenoxido donors H_5L^1 and H_5L^2 (H_5L^2 = 2-hydroxy-*N*-{2-hydroxy-4-[(2-hydroxybenzoyl)amino]butyl}benzamide). In these complexes, the ligands H_5L^1 and H_5L^2 act as fully deprotonated pentadentate ligands, $[L^1]^{5-}$ and $[L^2]^{5-}$; the noncoordinated amido oxygen atoms of these ligands are involved in hydrogen-bonding interactions.

[a] Inorganic Chemistry Department, Faculty of Chemistry, University of Bucharest,
23 Dumbrava Roşie, 020464 Bucharest, Romania
Fax: +40-21-3159249
E-mail: stoicescu.liliana@unibuc.ro
[b] CNRS, LCC (Laboratoire de Chimie de Coordination), Université de Toulouse, UPS, INPT,
205, route de Narbonne, 31077 Toulouse, France
Fax: +33-561-553003
E-mail: jean-pierre.tuchagues@lcc-toulouse.fr

The present work stems from our interest in studying the coordination behavior of the potentially pentaanionic, heptadentate ligands H_5L^1–H_5L^3 (shown below) (H_5L^3 = 2-hydroxy-*N*-{3-hydroxy-5-[(2-hydroxybenzoyl)amino] pentyl}benzamide) towards transition metals. Herein we describe the synthesis of a new potentially pentaanionic, heptadentate ligand that includes alkoxido, amido, and phenoxido donors, H_5L^3, and the synthesis, crystal structure and magnetic properties of copper(II), manganese(III), and iron(III) complexes of the potentially pentaanionic, heptadentate ligands H_5L^1 and H_5L^3: $[Cu_2(L^1)(OAc)Cs_2(MeOH)_2]_n$ (**1**), $[Mn_2(H_3L^1)_2(OMe)_2]\cdot 2MeOH$ (**2**), $[Fe_2(H_3L^1)_2(Hpz)_4](ClO_4)_2\cdot 2CH_3CN$ (**3**), and $[Fe_2(H_3L^3)_2(OMe)_2]\cdot 8MeOH$ (**4**).

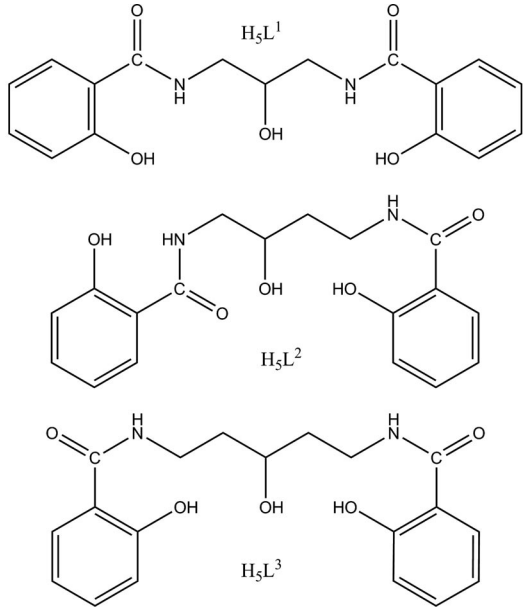

Results and Discussion

Synthesis

The ligands were synthesized according to a reported method[30,47] by condensation of phenylsalicylate with the corresponding 1,*n*-diamino-*n*′-hydroxyalkanes (*n*, *n*′ = 3, 2; 5, 3) in the presence of triethylamine in propan-2-ol. The ligand H_5L^3 is a new potentially pentaanionic, heptadentate ligand that includes alkoxido, amido, and phenoxido donors. We have previously reported that the reaction of dilute methanol solutions of $[Mn_3(\mu_3\text{-}O)(OAc)_6(H_2O)_3](OAc)\cdot 3H_2O$ and H_5L^1 in the presence of piperidine yields the complex $[Mn_2(L^1)(OAc)(MeOH)_4]$, and the reaction of dilute methanol solutions of $Mn(ClO_4)_2\cdot 6H_2O$, H_5L^1 or H_5L^2, and pyrazole in the presence of piperidine yields the complexes $[Mn_2(L^1)(pz)(MeOH)_4]\cdot 0.5MeOH$ and $[Mn_2(L^2)(pz)(MeOH)_4]$. Formation of these complexes involves full deprotonation of H_5L^1 and H_5L^2 to $[L^1]^{5-}$ and $[L^2]^{5-}$, respectively. As an extension of this work, we were dedicated to determine the products of similar reactions using other transition metals and/or ancillary ligands. The reaction of $Cu(OAc)_2\cdot H_2O$ with H_5L^1 in the presence of $CsOH\cdot H_2O$ forms blue crystals of complex **1**, $[Cu_2(L^1)(OAc)Cs_2(MeOH)_2]_n$, that have the dinucleating pentaanionic $[L^1]^{5-}$ and bridging acetato ligands. Complex **2**, $[Mn_2(H_3L^1)_2(OMe)_2]\cdot 2MeOH$, was prepared by reaction of dilute methanol solutions of $Mn(ClO_4)_2\cdot 6H_2O$ and H_5L^1 in the presence of sodium methoxide. Attempts to obtain the μ-alkoxido-μ-methoxido dinuclear manganese(III) complex incorporating $[L^1]^{5-}$ failed. Complex **3**, $[Fe_2(H_3L^1)_2(Hpz)_4](ClO_4)_2\cdot 2CH_3CN$, was prepared through reaction between $Fe(ClO_4)_2\cdot 6H_2O$, H_5L^1, and pyrazole in the presence of piperidine. Complex **4**, $[Fe_2(H_3L^3)_2(OMe)_2]\cdot 8MeOH$, was prepared by reaction of dilute methanol solutions of $Fe(OAc)_2$ and H_5L^3 in the presence of piperidine. Efforts to obtain the μ-alkoxido-μ-pyrazolato or the μ-alkoxido-μ-acetato iron(III) dinuclear complexes that incorporate the fully deprotonated ligands $[L^1]^{5-}$ and $[L^3]^{5-}$ have been unsuccessful to the best of our knowledge. Only complexes **3** and **4**, which incorporate the partially deprotonated ligands $[H_3L^1]^{2-}$ and $[H_3L^3]^{2-}$, were isolated. Complexes **3** and **4** are among the first structurally characterized Fe^{III} complexes of ligands that include two 2-hydroxybenzamido moieties.[25] Complexes **1** and **3** are soluble in MeOH, but complexes **2** and **4** are not soluble in common solvents.

Description of the Structures

$[Cu_2(L^1)(OAc)Cs_2(MeOH)_2]_n$ (1)

The molecule of **1** consists of anionic dicopper units $[Cu_2(L^1)(OAc)]^{2-}$ and $[Cs(MeOH)]^+$ cations. The molecular structure of the dianionic unit of **1** is shown in Figure 1 with selected bond lengths and angles listed in its caption. The two copper ions of the anionic, dinuclear unit $[Cu_2(L^1)(OAc)]^{2-}$ are bridged by the alkoxido oxygen atom of the pentaanionic ligand $[L^1]^{5-}$ and one acetato anion. The coordination geometry of the four-coordinate copper ions is distorted square planar.

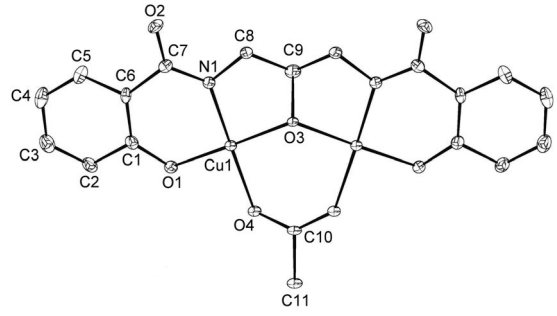

Figure 1. Plot of the anionic $[Cu_2(L^1)(OAc)]^{2-}$ unit of **1** at the 30% probability level with atom numbering. Hydrogen atoms are omitted for clarity. Selected bond lengths [Å] and angles [°]: Cu1–N1 1.905(4), Cu1–O1 1.900(4), Cu1–O3 1.921(2), Cu1–O4 1.970(4), $Cu1^{\#1}$–O3 1.921(2), N1–Cu1–O1 93.59(18), N1–Cu1–O3 86.30(19), N1–Cu1–O4 175.34(19), O1–Cu1–O4 88.71(16), O1–Cu1–O3 172.9(2), O3–Cu1–O4 91.92(18), C9–O3–Cu1 110.14(16), C9–O3–$Cu1^{\#1}$ 110.14(16), $Cu1^{\#1}$–O3–Cu1 136.5(3). Symmetry operation used to generate equivalent atoms: #1: *x*, *–y* + 1/2, *z*.

Each copper ion is coordinated by phenoxido oxygen, amido nitrogen and alkoxido oxygen donor atoms of $[L^1]^{5-}$ and by one acetato oxygen atom (1.90–1.97 Å). The bond lengths are in the range of those reported for other doubly bridged μ-alkoxido-μ-acetato dinuclear copper(II) complexes.[48–50] The ligand is almost planar, the angle between the phenyl rings being 12.6°. The bonding geometry around the alkoxido oxygen atom O3 is planar; the sum of the three bond angles around O3 is 357°. The intramolecular Cu···Cu separation in **1** [3.5681(8) Å] is longer than those found in $[Cu_2(L')(OAc)]\cdot MeOH$ [3.495(2) Å][49] and $[Cu_2(L')(CH_2ClCOO)MeOH]\cdot MeOH$ [3.514(1) Å][50] (H_3L' is the Schiff base ligand 2-[({2-hydroxy-3-[(2-hydroxybenzylidene)amino]propyl}imino)methyl]phenol). The Cu–$O_{alkoxido}$–Cu angle in **1** [136.5(3)°] is larger than the corresponding angle reported for $[Cu_2(L')(OAc)]\cdot MeOH$ [134.5(4)°][49] and for $[Cu_2(L')(CH_2ClCOO)MeOH]\cdot MeOH$ [132.7(2)°],[50] and the dihedral angle between the copper coordination planes is 13.7°.

The anionic $[Cu_2(L^1)(OAc)]^{2-}$ and cationic $[Cs(MeOH)]^+$ units are linked through a bridging acetato and the phenoxido oxygen and amido oxygen donor atoms of $[L^1]^{5-}$ to yield a 2D network (Figure 2). The cesium cations are hexacoordinate in a distorted trigonal-prismatic environment. Each cesium cation is coordinated to three different $[Cu_2(L^1)(OAc)]^{2-}$ units through a phenoxido oxygen of a dianionic $[Cu_2(L^1)(OAc)]^{2-}$ unit and through two amido oxygen donor atoms from different dianionic $[Cu_2(L^1)(OAc)]^{2-}$ units. The three remaining sites are occupied by an acetato oxygen and two methanol oxygen donor atoms. The acetato anion displays an unusual μ_4-η^2-η^2 coordination mode[51,52] and bridges two copper and two cesium ions. Each methanol oxygen atom bridges two cesium ions. Cs–O bonding interactions are strong, and all Cs–O distances [2.999(4)–3.279(4) Å] are well within the range reported in literature.[53] Each dinuclear copper(II) complex anion is in turn surrounded by four cesium ions. The shortest Cs···Cs separation is 4.4184(5) Å.

Although the hydrogen atom could not be located on atom O5 of the methanol molecule, the short O5···O2 distance (2.654 Å) strongly suggests an $O_{methanol}$–H···O_{amido} hydrogen bond. π–π stacking interactions are absent, but electrostatic interactions between the cesium ions and the phenyl rings are likely to operate. The Cs–C bond lengths range from 3.515 to 3.667 Å and are slightly longer than those reported for a complex involving interactions between the cesium ions and the imidazolate ring (3.323–3.607 Å).[54]

$[Mn_2(H_3L^1)_2(OMe)_2]\cdot 2MeOH$ (2)

The molecular structure of **2** is shown in Figure 3 with selected bond lengths and angles listed in its caption. The molecular structure of the dinuclear complex **2** shows that two manganese ions are bridged by two tetradentate $[H_3L^1]^{2-}$ ligands and two methoxido anions. The two amido oxygen and the two phenoxido oxygen atoms of each ligand

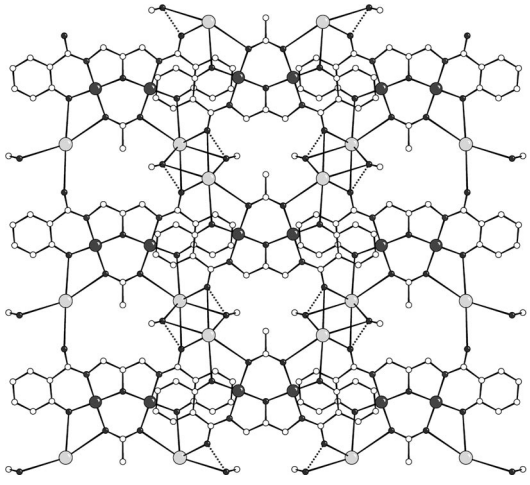

Figure 2. View of the crystal packing of **1** in a plane perpendicular to *a*. Hydrogen atoms are omitted for clarity. Selected bond lengths [Å] and angles [°]: Cs1–O1 2.999(4), Cs1–O4 3.139(4), Cs1–O5 3.000(5), Cs1–$O2^{\#4}$ 3.090(4), Cs1–$O2^{\#3}$ 3.279(4), $Cs1^{\#4}$–O2 3.090(4), Cs1–$O5^{\#2}$ 3.267(5), $Cs1^{\#2}$–O5 3.267(5), $Cs1^{\#5}$–O2 3.279(4), Cu1···Cs1 4.1096(7), O1–Cs1–$O2^{\#4}$ 79.51(12), O1–Cs1–O4 52.26(10), O1–Cs1–O5 118.91(13), O1–Cs1–$O5^{\#2}$ 111.44(12), O1–Cs1–$O2^{\#3}$ 168.01(12), $O2^{\#4}$–Cs1–O4 107.50(11), $O2^{\#4}$–Cs1–$O5^{\#2}$ 49.26(11), $O2^{\#4}$–Cs1–$O2^{\#3}$ 92.20(9), O4–Cs1–$O2^{\#3}$ 123.81(10), O4–Cs1–$O5^{\#2}$ 156.39(11), O5–Cs1–O4 85.41(13), O5–Cs1–$O2^{\#4}$ 73.90(12), O5–Cs1–$O2^{\#3}$ 49.77(12), $O5^{\#2}$–Cs1–$O2^{\#3}$ 68.03(11), O5–Cs1–$O5^{\#2}$ 90.45(13), Cs1–O5–$Cs1^{\#2}$ 89.55(13), $Cs1^{\#4}$–O2–$Cs1^{\#5}$ 87.80(9). Symmetry operations used to generate equivalent atoms: #2: $-x + 1, -y, -z + 1$; #3: $x, y, z + 1$; #4: $-x + 1, -y, -z$; #5: $x, y, z - 1$.

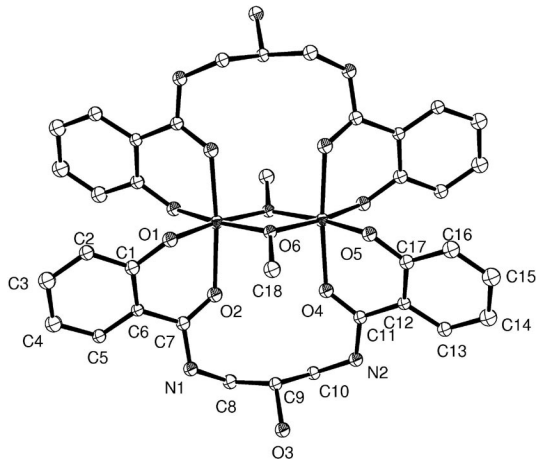

Figure 3. Plot of $[Mn_2(H_3L^1)_2(OMe)_2]\cdot 2MeOH$ (**2**) at the 30% probability level with atom numbering. Hydrogen atoms and methanol solvate are omitted for clarity. Selected bond lengths [Å] and angles [°]: Mn1–O1 1.899(5), Mn1–O2 2.187(5), Mn1–$O4^{\#1}$ 2.125(5), Mn1–$O5^{\#1}$ 1.858(5), Mn1–O6 1.942(5), Mn1–$O6^{\#1}$ 1.954(5), O1–Mn1–O2 85.7(2), O1–Mn1–$O4^{\#1}$ 91.3(2), O1–Mn1–$O5^{\#1}$ 94.1(2), O1–Mn1–O6 94.5(2), O1–Mn1–$O6^{\#1}$ 171.1(2), O2–Mn1–$O4^{\#1}$ 174.31(19), O2–Mn1–$O5^{\#1}$ 89.8(2), O2–Mn1–O6 92.97(19), O2–Mn1–$O6^{\#1}$ 91.25(19), $O4^{\#1}$–Mn1–$O5^{\#1}$ 85.6(2), $O4^{\#1}$–Mn1–$O6^{\#1}$ 92.43(19), $O4^{\#1}$–Mn1–O6 92.08(19), $O5^{\#1}$–Mn1–O6 171.2(2), $O5^{\#1}$–Mn1–$O6^{\#1}$ 94.3(2), $O6^{\#1}$–Mn1–O6 77.3(2), $Mn1^{\#1}$–O6–Mn1 102.7(2), $Mn1^{\#1}$–Mn1–O1 133.17(15), $Mn1^{\#1}$–Mn1–O2 92.70(14), $Mn1^{\#1}$–Mn1–O6 38.77(13), $O4^{\#1}$–Mn1–$Mn1^{\#1}$ 92.89(14), $Mn1^{\#1}$–Mn1–$O5^{\#1}$ 132.74(16), $Mn1^{\#1}$–Mn1–$O6^{\#1}$ 38.49(14). Symmetry operation used to generate equivalent atoms: #1: $-x + 2, -y, -z$.

are coordinated to two different manganese ions. The coordination polyhedra of the Mn^{III} ions may be described as elongated octahedra. The axial Mn–O_{amido} bonds [2.125(5) and 2.187(5) Å] are significantly longer than the equatorial Mn–$O_{methoxido}$ and Mn–$O_{phenoxido}$ bonds [1.899(5)–1.954(5) Å]. The Mn–O bond lengths in the equatorial plane are similar to Mn^{III}–O bond lengths in reported complexes.[55] The two Mn–$O_{methoxido}$ bond lengths are nearly identical, 1.942(5) Å and 1.954(5) Å. The two Mn^{III} ions and the two bridging methoxido oxygen atoms form a perfect plane, with Mn–$O_{methoxido}$–Mn and $O_{methoxido}$–Mn–$O_{methoxido}$ bridging angles of 102.7(2)° and 77.3(2)°, respectively. These angles are similar to those reported for other $Mn_2(\mu\text{-}OMe)_2$ complexes.[56] The intramolecular Mn···Mn distance [3.044(2) Å] in **2** falls in the range observed for the reported $Mn_2(\mu\text{-}OMe)_2$ complexes.[55–57]

The crystal packing of **2** consists of 2D sheets, which result from hydrogen-bonding interactions between the alcohol oxygen, amido nitrogen, and amido oxygen atoms of the $[H_3L^1]^{2-}$ ligand from adjacent dinuclear molecules of **2** (Figure 4). The methanol lattice molecules are also involved in strong N_{amido}–H···$O_{methanol}$ hydrogen bonds (D–H···A, *d* [Å], ∠ [°]: N2–H2···O3$^{\#2}$, 2.87, 148; O3–H3···O1$^{\#3}$, 2.76, 148; N1–H1···O7$^{\#1}$, 2.86, 161; symmetries #1: $-x + 1$, $+y - 1/2$, $-z + 1/2$; #2: $-x + 2$, $-y - 1$, $-z$; #3: $-x + 2$, $+y - 1/2$, $-z + 1/2$).

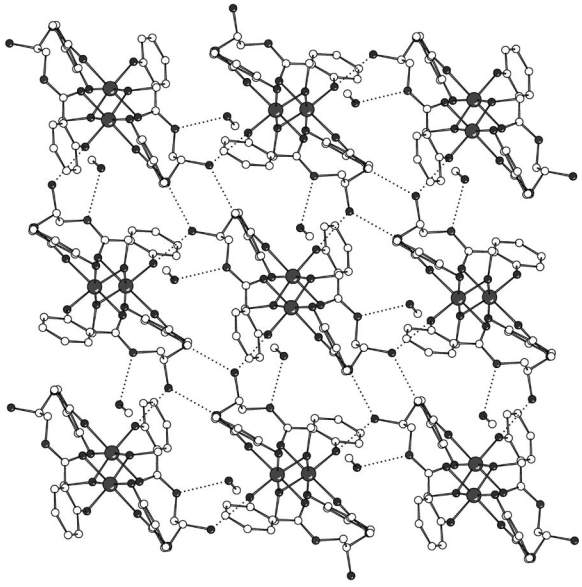

Figure 4. Crystal packing diagram of $[Mn_2(H_3L^1)_2(OMe)_2]\cdot 2MeOH$ (**2**): view perpendicular to the *a* axis.

$[Fe_2(H_3L^1)_2(Hpz)_4](ClO_4)_2\cdot 2CH_3CN$ (3)

The molecular structure of **3** consists of a dinuclear $[Fe_2(H_3L^1)_2(Hpz)_4]^{2+}$ cation shown in Figure 5, two perchlorate anions, and two acetonitrile molecules as crystallization solvent. In the dinuclear $[Fe_2(H_3L^1)_2(Hpz)_4]^{2+}$ cation, the Fe^{III} ions bridged by two tetradentate $[H_3L^1]^{2-}$ ligands assume a distorted octahedral coordination geometry. Each Fe^{III} ion is in a distorted octahedral ligand environment that includes two nitrogen atoms from two *cis* Hpz molecules, two amido oxygen atoms, and two phenoxido oxygen atoms from two tetradentate dianionic $[H_3L^1]^{2-}$ ligands, with bond lengths similar to those reported for other complexes with a N_2O_4-type hexacoordination of the Fe^{III} ions:[58,59] Fe–N 2.111(6) and 2.143(6) Å, Fe–O_{amido} 2.001(4) and 2.009(4) Å, Fe–$O_{phenoxido}$ 1.904(4) and 1.943(4) Å. The intramolecular Fe···Fe distance is very large [7.926(3) Å]. Selected bond lengths and angles are listed in the caption of Figure 5.

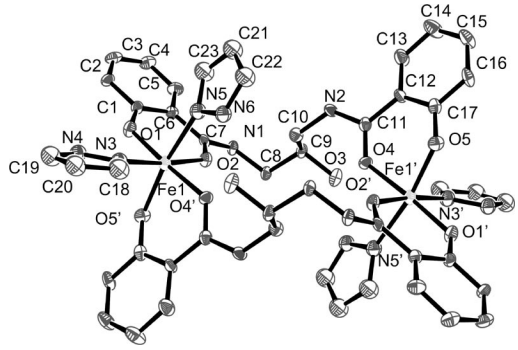

Figure 5. Plot of $[Fe_2(H_3L^1)_2(Hpz)_4](ClO_4)_2\cdot 2CH_3CN$ (**3**) at the 30% probability level with atom numbering. Hydrogen atoms, perchlorate anions, and acetonitrile solvate are omitted for clarity. Selected bond lengths [Å] and angles [°]: Fe1–O1 1.904(4), Fe1–O2 2.001(4), Fe1–O4$^{\#1}$ 2.009(4), Fe1–O5$^{\#1}$ 1.943(4), Fe1–N3 2.111(6), Fe1–N5 2.143(6), O1–Fe1–O2 87.83(16), O1–Fe1–N3 88.56(18), O1–Fe1–N5 94.16(19), O1–Fe1–O4$^{\#1}$ 176.6(2), O1–Fe1–O5$^{\#1}$ 96.30(18), O2–Fe1–N3 174.57(19), O2–Fe1–O4$^{\#1}$ 90.79(16), O2–Fe1–N5 86.76(19), N3–Fe1–N5 89.5(2), O4$^{\#1}$–Fe1–N3 92.59(18), O4$^{\#1}$–Fe1–N5 82.65(18), O5$^{\#1}$–Fe1–O2 94.02(18), O5$^{\#1}$–Fe1–N3 90.4(2), O5$^{\#1}$–Fe1–O4$^{\#1}$ 86.90(16), O5$^{\#1}$–Fe1–N5 169.53(17). Symmetry operation used to generate equivalent atoms: #1: $-x + 1$, $-y$, $-z + 1$.

The crystal packing of **3** consists of 1D infinite chains (Figure 6), which result from intermolecular hydrogen-bonding interactions involving amido nitrogen and phenoxido oxygen atoms from adjacent dinuclear cations of **3**. The noncoordinated alcohol oxygen atoms participate in intramolecular hydrogen bonds. The acetonitrile lattice molecules and the perchlorate anions are also involved in strong hydrogen bonds (D–H···A, *d* [Å], ∠ [°]: N1–H1···O5$^{\#2}$ 2.92, 153; N6–H6···O3$^{\#4}$ 2.85, 169; O3–H3···O8$^{\#1}$ 2.72, 158; N2–H2···N7 2.89, 152; symmetries #1: *x*, $y - 1$, *z*; #2: $x + 1$, *y*, *z*; #4: $-x + 1$, $-y$, $-z + 1$). Taking into account the very

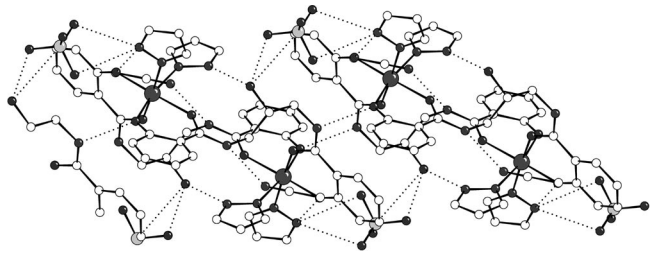

Figure 6. View of the crystal packing of **3** in a plane perpendicular to *c*, showing 1D chains of hydrogen-bonded molecules.

large Fe···Fe intramolecular distance, it is most likely that these hydrogen-bonding interactions play an important role in the stabilization of the crystal molecular structure of complex **3**.

[$Fe_2(H_3L^3)_2(OMe)_2$]·8MeOH (4)

The molecular structure of **4** is shown in Figure 7 with selected bond lengths and angles listed in its caption. The molecular structure of the dinuclear complex **4** shows that the two iron ions are bridged by two tetradentate $[H_3L^3]^{2-}$ ligands and two methoxido groups. Each ligand is chelated to both iron centers through one amido and one phenoxido oxygen atoms [1.956(2)–2.058(3) Å]. The two Fe–$O_{methoxido}$ bond lengths are almost equal [1.989(2) Å and 1.996(3) Å]. The Fe–$O_{methoxido}$–Fe and $O_{methoxido}$–Fe–$O_{methoxido}$ bridging angles are 104.17(11)° and 75.83(11)°, respectively. These angles are typical of a four-membered Fe_2O_2 ring.[25,60–62] The coordination geometry around the iron(III) ions is distorted octahedral. The largest deviations are found for O6–Fe1–O6 [75.83(11)°] and O1–Fe1–O6 [165.04(11)°] and may be attributed to the restriction imposed by the four-membered Fe_2O_2 ring in the bridging region.[55,61] The intramolecular Fe···Fe distance [3.1443(9) Å] in **4** is similar to that observed for several reported $Fe_2(\mu\text{-}OMe)_2$ complexes.[25,60–62]

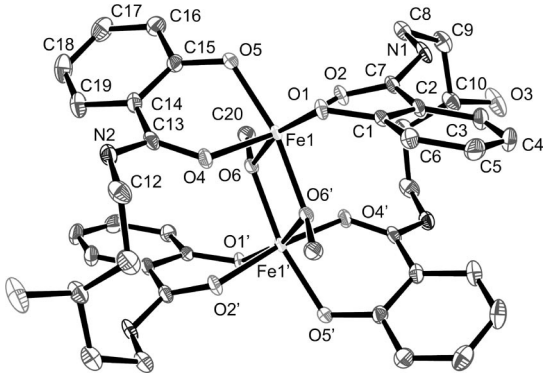

Figure 7. Plot of $[Fe_2(H_3L^3)_2(OMe)_2]$·8MeOH (**4**) at the 30% probability level with atom numbering. Hydrogen atoms and methanol solvate are omitted for clarity. Selected bond lengths [Å] and angles [°]:Fe1–O1 1.956(2), Fe1–O2 2.042(3), Fe1–O4 2.058(3), Fe1–O5 1.971(3), Fe1–O6 1.989(2), Fe1–$O6^{\#1}$ 1.996(3), O1–Fe1–O2 85.09(10), O1–Fe1–O4 89.20(11), O1–Fe1–O5 98.84(11), O1–Fe1–O6 165.04(11), O1–Fe1–$O6^{\#1}$ 92.81(11), O2–Fe1–O4 169.86(11), O2–Fe1–O5 88.40(11), O2–Fe1–O6 87.12(10), O2–Fe1–$O6^{\#1}$ 99.15(11), O4–Fe1–O5 84.20(11), O4–Fe1–O6 100.23(10), O4–Fe1–$O6^{\#1}$ 89.48(11), O5–Fe1–O6 93.68(11), O5–Fe1–$O6^{\#1}$ 166.64(10), O6–Fe1–$O6^{\#1}$ 75.83(11), Fe1–O6–$Fe1^{\#1}$ 104.17(11). Symmetry operation used to generate equivalent atoms: #1: $-x + 1, -y + 2, -z + 1$.

The crystal packing of **4** consists of 2D sheets parallel to *b*, which result from hydrogen bonds that develop along the *a* and *c* directions (Figure 8). Four methanol lattice molecules are involved in $O_{methanol}$–H···$O_{phenoxido}$ and N_{amido}–H···$O_{methanol}$ hydrogen bonds (D–H···A, *d* [Å], ∠ [°]: O20A–H20D···$O1^{\#4}$, 2.69, 153; O100–H100···$O5^{\#5}$, 2.67, 151; N2–H2···$O20A^{\#1}$, 2.84, 165; symmetries #1: $x + 1, y, z$; #4: $-x + 1, -y + 2, -z + 1$; #5: $x - 1, y, z$), and two lattice methanol molecules are involved in $O_{methanol}$–H···$O_{methanol}$ hydrogen bonds (D–H···A, *d* [Å], ∠ [°]: O22–H22···$O23^{\#3}$, 2.68, 149; symmetry #3: $x - 1, y, z + 1$). The amido nitrogen atom and the alcohol oxygen atom from adjacent dinuclear molecules of **4** are involved in N_{amido}–H···$O_{alcohol}$ hydrogen bonds (D–H···A, *d* [Å], ∠ [°]: N1–H1···$O3^{\#2}$, 2.87, 162; symmetry #2: $x, -y + 2, -z + 2$). The alcohol oxygen atom is also involved in a strong $O_{alcohol}$–H···$O_{methanol}$ hydrogen bond (D–H···A, *d* [Å], ∠ [°]: O3–H3B···O100, 2.69, 151).

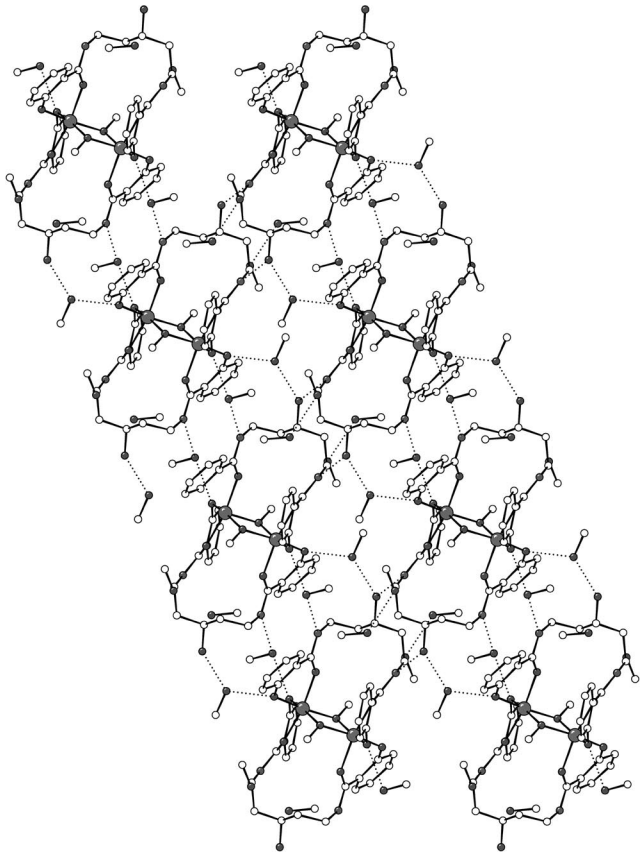

Figure 8. Crystal packing diagram of $[Fe_2(H_3L^3)_2(OMe)_2]$·8MeOH (**4**): view perpendicular to the *b* axis.

UV/Vis spectroscopy

The dinuclear Cu^{II} complex **1** shows three absorption bands in the region 338–629 nm. The low-energy absorption band (629 nm) is assigned to a Cu^{II} d–d transition, and the high-energy absorption band (338 nm) is ligand related. The absorption band at 377 nm may be assigned to a charge-transfer from the bridging alkoxido oxygen atom to the copper(II) ion.[68]

The dinuclear Mn^{III} complex **2** exhibits a solid-state electronic spectrum typical of a high-spin d^4 electronic configuration. The spectrum is characterized by several absorption bands in the region 347–658 nm. The 347 nm absorption band (present in the spectrum of H_5L^1) is ligand related. The absorption band at 440 nm is assigned to a LMCT transition from the phenoxido oxygen atom to the Mn^{III} ion. The low-energy absorption bands (549–658 nm) are as-

signed to Mn^{III} d–d transitions. These spectral features are consistent with the elongated octahedral environment of Mn^{III} ions.[30]

The spectra of the dinuclear Fe^{III} complexes **3** and **4** are characterized by two absorption bands in the region 348–584 nm. The high-energy absorption band at 359 nm for **3** and 348 nm for **4** is ligand related. The broad absorption maximum in the visible region is due to LMCT transitions and is responsible for the dark violet–reddish color of **3** (λ_{max} at 584 nm) and orange color of **4** (λ_{max} at 505 nm).[45,25]

Magnetic properties

The magnetic susceptibility of complexes **1**–**4** has been measured in the 1.8–300 K temperature range, under an applied magnetic field of 0.1 T. In agreement with the molecular structure described above, the $\chi_M T$ product of compounds **1**, **2**, and **4** decreases upon cooling (Figures 9 and 10), which indicates the operation of antiferromagnetic interactions between the metal centers of the dinuclear structures of **1**, **2**, and **4**. As expected from the large distance (7.9 Å) and the absence of an efficient magnetic interaction pathway between its iron centers, the $\chi_M T$ product of the dinuclear compound **3** is constant over the whole temperature range, with the exception of a minute decrease below 4 K, which can be attributed to the zero-field splitting (zfs) of the Fe^{III} single ion. Consequently, the magnetic behavior of this simple paramagnetic species will not be discussed further.

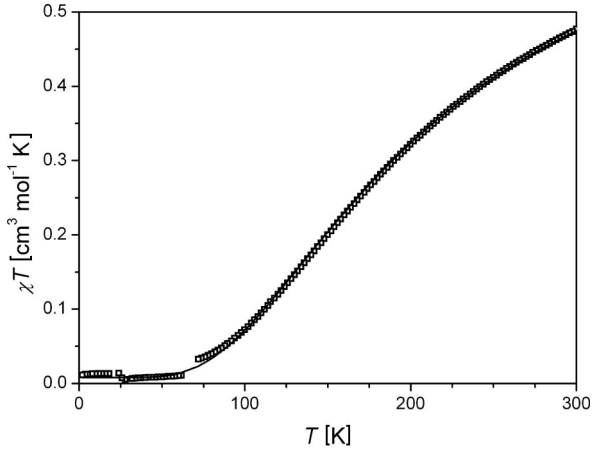

Figure 9. $\chi_M T$ vs. T data for $[Cu_2(L^1)(OAc)Cs_2(MeOH)_2]_n$ (**1**). The squares are measured data, and the line is the best fit on the basis of the Hamiltonian described in the text.

While in the dinuclear copper(II) compound **1**, as in most complexes of the amido ligands in this series,[30] $[L^1]^{5-}$ is dinucleating through its central alkoxido oxygen atom; its partly protonated $[H_3L^1]^{2-}$ form does not participate in transmitting magnetic interaction in **2** nor does the parent $[H_3L^3]^{2-}$ ligand in **4**. In the latter two complexes, magnetic interactions are mediated by two methoxido bridges; however, the Mn^{III} (Fe^{III}) centers of complex **2** (**4**) are also bridged by the –OC(NH)–R–C(NH)O– central part of

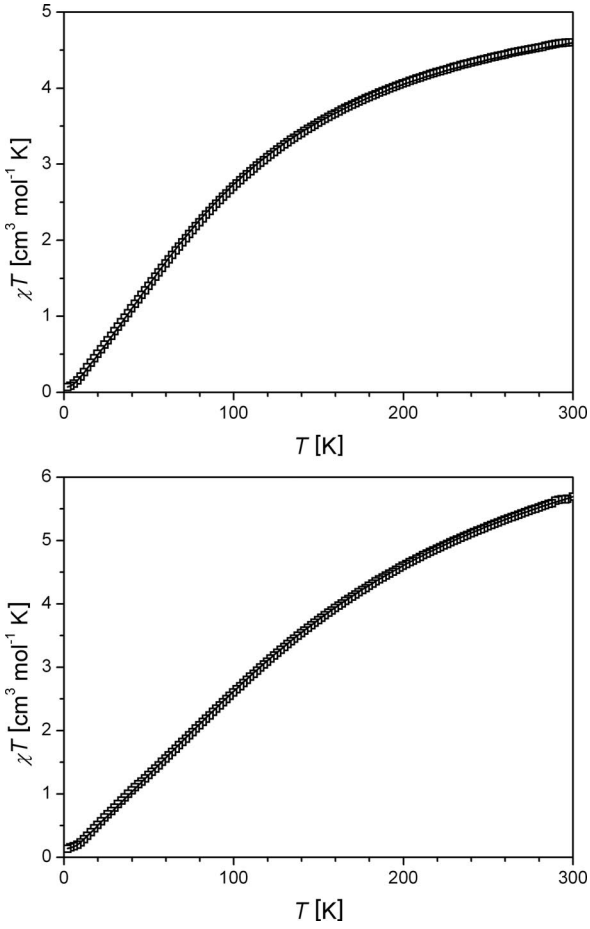

Figure 10. $\chi_M T$ vs. T data for $[Mn_2(H_3L^1)_2(OMe)_2]\cdot 2MeOH$ (**2**, top) and $[Fe_2(H_3L^3)_2(OMe)_2]\cdot 8MeOH$ (**4**, bottom). The squares are measured data, and the lines are the best fits on the basis of the Hamiltonian described in the text.

both $[H_3L^1]^{2-}$ ($[H_3L^3]^{2-}$) polydentate ligands. Magnetic interactions are thus mediated through similar pathways in **2** and **4**, but very different pathways in **2** and **4** relative to **1**.

The magnetic susceptibility of **1**, χ_M, increases from 1.59×10^{-3} cm^3 mol^{-1} at 300 K to a broad maximum of 1.66×10^{-3} cm^3 mol^{-1} at about 235 K, which is typical of antiferromagnetic interactions. The magnetic susceptibility then slowly decreases down to 2×10^{-4} cm^3 mol^{-1} at 28 K before increasing up to 5.7×10^{-3} cm^3 mol^{-1} at 2 K. While the χ_M value at room temperature corresponds to a magnetic moment (1.95 BM) lower than expected for two noninteracting Cu^{II} cations (2.5 BM for $g = 2$), the low temperature paramagnetic tail is characteristic of the presence of a small percentage of paramagnetic impurity. In order to fit these experimental data, a simple system of two exchange-coupled Cu^{II} ($S = 1/2$) cations was considered ($\hat{H} = -2J\hat{S}_{Cu1}\hat{S}_{Cu2}$).[63] Attempts to fit the data with this simple model yielded satisfactory results when also taking into account the presence of a small fraction of paramagnetic impurity (p%). The parameter values for the best fit, shown as a solid line in Figure 9, are: $J = -132(1)$ cm^{-1}, $g = 2.024(4)$, $p = 0.5$%. The agreement factor $R = \Sigma[(\chi_M T)_{obs} - (\chi_M T)_{calc}]^2/\Sigma[(\chi_M T)_{obs}]^2 = 2 \times 10^{-4}$.

The $|2J|$ value for **1** (264 cm^{-1}) is at the upper end of those reported for dinuclear complexes in which the copper(II) centers are doubly bridged by similar alkoxido and carboxylato oxygen donor atoms. The reported $|2J|$ values are in the 38–280,[48] 160–170,[49] and 96.4–173.4 cm^{-1}[50] ranges. The key factors that are usually considered to govern the nature and strength of superexchange magnetic interactions in such doubly bridged Cu^{II} dinuclear complexes are the Cu–$O_{alkoxido}$–Cu angle, the distortion from trigonal-planar toward pyramidal bonding around $O_{alkoxido}$ (also reflected by the dihedral angle between the copper coordination planes), and the Cu···Cu distance.[48–50] In **1**, the Cu–$O_{alkoxido}$–Cu angle is larger than in previously reported examples,[48–50] the bonding geometry around the alkoxido oxygen atom O3 is close to planarity, the sum of the three bond angles around O3 is 357° (small dihedral angle of 13.7° between the copper coordination planes), and the intramolecular Cu···Cu separation (3.568 Å) is at the upper end of those previously reported.[48–50] The values of these structural parameters support a fairly strong antiferromagnetic interaction, in agreement with the rather large $|2J|$ value (264 cm^{-1}) evaluated for **1**.

The magnetic susceptibility, χ_M, of **2** (**4**) increases from 1.53×10^{-2} $cm^3 mol^{-1}$ (1.90×10^{-2}) at 300 K to a maximum of 2.83×10^{-2} $cm^3 mol^{-1}$ (2.61×10^{-2}) at 63 K (84), which is typical of antiferromagnetic interactions. The magnetic susceptibility then slowly decreases down to 1.93×10^{-2} $cm^3 mol^{-1}$ (2.38×10^{-2}) at 5.8 K (9.8) before increasing up to 3.37×10^{-2} $cm^3 mol^{-1}$ (6.59×10^{-2}) at 2 K. While the χ_M values at room temperature correspond to magnetic moments (**2**, 6.08; **4**, 6.82 BM) lower than expected for two noninteracting Mn^{III} (≈7 BM for $g = 2$) and Fe^{III} cations (≈8.4 BM for $g = 2$), the low-temperature paramagnetic tails are characteristic of the presence of a small percentage of paramagnetic impurity.

In order to fit these experimental data, a simple system of two exchange-coupled Mn^{III} ($S = 2$) cations, (Fe^{III}, $S = 5/2$) was considered ($\hat{H} = -2J\hat{S}_{M1}\hat{S}_{M2}$) as a first step.[63] Attempts to fit the data with this simple model yielded only average results with discrepancies at lower temperatures for both complexes **2** and **4**, even when taking into account the presence of a small fraction of paramagnetic impurity (p%). The axially elongated octahedral coordination spheres of the Mn^{III} (**2**) and Fe^{III} (**4**) centers led us to assume that zero-field splitting effects might be operative. The introduction of a zero-field splitting term D, common for both metal sites ($D_1 = D_2 = D$), brought about significant improvements to the fits of **2** and **4**. The implemented Hamiltonian was: $\hat{H} = -2J\hat{S}_{M1}\hat{S}_{M2} + D(\hat{S}_{zM1}{}^2 + \hat{S}_{zM2}{}^2)$.[64] This model reproduces the experimental curves very well; however there are small discrepancies at low temperature, which may result from simultaneous operation of intermolecular interactions between adjacent dinuclear molecules yielding 2D sheets (see Description of Structures). Since introduction of an intermolecular interaction according to the mean-field Hamiltonian[65] $\hat{H} = -2zJ\langle S_z\rangle\hat{S}_z$ affords a marginal improvement to the fits of **2** and **4**, only zero-field splittings were considered in order to avoid overparametrization. The parameter values for the best fits, shown as solid lines in Figure 10, are: $J = -10.7(3)$ cm^{-1}, $D = -5.3(3)$ cm^{-1}, $g = 1.973(6)$, $p = 0.6$%, $R = 1.0\ 10^{-4}$ (**2**) and $J = -12.1(4)$ cm^{-1}, $D = -3.0(2)$ cm^{-1}, $g = 1.960(6)$, $p = 0.8$%, $R = 1.5\ 10^{-4}$ (**4**).

The few previously reported $-2J$ values for dinuclear complexes in which the manganese(III) centers are doubly bridged by similar methoxido oxygen atoms are 20.7,[53] 16.4 and 23.6,[56] and –19.7 cm^{-1}.[57] With the exception of the later (ferromagnetic), which belongs to an asymmetric complex in which the Mn^{III} ions are in differently distorted octahedra with Jahn–Teller axes at an angle of ca. 100°, the $-2J$ value for **2** (21.4 cm^{-1}) is in the range of those already reported. Accordingly, the geometric parameters of **2** significant for magneto-structural correlations Mn–$O_{methoxido}$–Mn = 102.7°, planar Mn_2O_2 ring, Mn···Mn = 3.044 Å are similar to those reported in the literature (Mn–$O_{methoxido}$–Mn = 102.5°, planar Mn_2O_2 ring, Mn···Mn = 3.00 Å;[55] Mn–$O_{methoxido}$–Mn = 102.5°, planar Mn_2O_2 ring, Mn···Mn = 3.038 Å).[56] Extension of this comparison to other dinuclear complexes in which the Mn^{III} cations are doubly bridged by other alkoxido oxygen atoms shows that the $-2J$ value for **2** (21.4 cm^{-1}) is at the upper end of the reported range.[30]

In agreement with the significant Jahn–Teller axial elongation of the Mn^{III} coordination octahedron along the Mn–O_{amido} bonds (2.125 and 2.187 Å; 1.899–1.954 Å for the equatorial Mn–$O_{methoxido}$ and Mn–$O_{phenoxido}$ bonds), a rather large negative value was found for $D = (-5.3$ $cm^{-1})$. This value is, however, of the same order of magnitude as the reported single ion zfs D parameters in Mn^{III} complexes.[30,57,66]

The few previously reported $-2J$ values for dinuclear complexes in which the iron(III) centers are doubly bridged by similar methoxido or ethoxido oxygen atoms are 32.6,[61a] 30.8,[61b] and 22 cm^{-1}.[67] The $-2J$ value for **4** (24.2 cm^{-1}) is in the range of those already reported. Accordingly, the geometric parameters of **4** significant for magneto-structural correlations Fe–$O_{methoxido}$–Fe = 104.2°, planar Fe_2O_2 ring, Fe···Fe = 3.145 Å are similar to those reported in the literature (Fe–$O_{alkoxido}$–Fe = 103 and 104.3°, planar Fe_2O_2 ring in one complex and a dihedral angle of 169° between the Fe–O–O planes in the other, Fe···Fe = 3.106 and 3.144 Å[59]).

A zfs D value of –3.0 cm^{-1} was found for complex **4**. The sign of D cannot be safely determined from magnetic susceptibility data alone, therefore sign attribution is tentative, and we only discuss the absolute value $|D| = 3$ cm^{-1}. This zfs may be attributed to the axial elongation of the Fe^{III} coordination octahedron along the Fe–O_{amido} bonds (2.042 and 2.058 Å; 1.956–1.996 Å for the equatorial Fe–$O_{methoxido}$ and Fe–$O_{phenoxido}$ bonds). The 3 cm^{-1} absolute value is in the range of those reported for the single ion zfs D parameter in octahedral Fe^{III} complexes.[66]

Conclusions

In this paper we report on the preparation of one novel multidentate ligand and four novel transition-metal com-

plexes. H_5L^3 (2-hydroxy-*N*-{3-hydroxy-5-[(2-hydroxybenzoyl)amino]pentyl}benzamide) extends the family (H_5L^1–H_5L^2)[30] of potentially pentaanionic, heptadentate ligands that include alkoxido, amido, and phenoxido donors and incorporate two 2-hydroxybenzamide moieties. We aimed to explore the coordination ability and versatility of the H_5L^1–H_5L^3 family of ligands not only toward manganese, but also toward other transition-metal ions. In this respect, we have prepared four complexes involving copper(II), manganese(III), and iron(III): $[Cu_2(L^1)(OAc)Cs_2(MeOH)_2]_n$ (**1**), $[Mn_2(H_3L^1)_2(OMe)_2]\cdot 2MeOH$ (**2**), $[Fe_2(H_3L^1)_2(Hpz)_4](ClO_4)_2\cdot 2CH_3CN$ (**3**), and $[Fe_2(H_3L^3)_2(OMe)_2]\cdot 8MeOH$ (**4**) and explored their structural and electronic properties.

Complex **1** is an original complex containing an acetate ion that displays an unusual μ_4-η^2-η^2 coordination mode and bridges two copper ions and two cesium ions. In this complex, H_5L^1 is fully deprotonated to $[L^1]^{5-}$ and acts as a dinucleating pentadentate ligand toward Cu^{II}. The anionic $[Cu_2(L^1)(OAc)]^{2-}$ and cationic $[Cs(MeOH)]^+$ units are linked through a bridging acetato and phenoxido oxygen and amido oxygen donor atoms of $[L^1]^{5-}$ to form a remarkable 2D network. The large $Cu–O_{alkoxido}–Cu$ angle mediates one of the larger antiferromagnetic interactions (J = –132 cm^{-1}) ever reported for similarly bridged dinuclear Cu^{II} complexes.

At variance with this coordination mode, H_5L^1 is partially deprotonated to $[H_3L^1]^{2-}$ and acts as a bridging tetradentate ligand toward Mn^{III} in **2** and toward Fe^{III} in **3**: the Mn^{III} (Fe^{III}) centers of complex **2** (**3**) are bridged by the –OC(NH)–R–C(NH)O– central part of two $[H_3L^1]^{2-}$ polydentate ligands. However, while the Mn^{III} centers of complex **2** are additionally bridged by two methoxido anions to yield a 3.044 Å Mn···Mn separation and mediating magnetic interactions (J = –10.7 cm^{-1}), the absence of bridging methoxido anions between the Fe^{III} centers of **3** results in a large Fe···Fe separation (7.93 Å) and the absence of magnetic interactions. H_5L^3 is partially deprotonated to $[H_3L^3]^{2-}$ in **4** and, similarly to the cases of **2** and **3**, the Fe^{III} centers are bridged by the –OC(NH)–R–C(NH)O– central part of two $[H_3L^3]^{2-}$ polydentate ligands; two methoxo bridges yield a 3.144 Å Fe···Fe separation and mediate magnetic interactions (J = –12.1 cm^{-1}), similarly to the case of **2**.

The supramolecular structure of **2** and **4** consists of 2D sheets, which differs from the supramolecular structure of **3** (consists of 1D infinite chains); in all three complexes a dense network of intermolecular hydrogen-bonding interactions is responsible for the observed crystal packing.

Experimental Section

Materials: All reagents and solvents used in this study are commercially available (Aldrich or Fluka) and were used without further purification. All syntheses were carried out in aerobic conditions.

CAUTION! Perchlorate salts of metal complexes with organic ligands are potentially explosive. Only small quantities of compounds should be prepared, and they should be handled with much care!

H_5L^1: This ligand was synthesized according to a reported method.[30]

H_5L^3: 1,5-Diaminopentan-3-ol dihydrochloride was synthesized according to a reported method.[68] 1,5-Diaminopentan-3-ol was obtained by reaction of its hydrochloride salt (1.720 g, 9 mmol) with potassium *tert*-butoxide (2.020 g, 18 mmol) in ethanol (30 mL). The KCl precipitate was filtered off, and the filtrate was concentrated under vacuum at about 1/3 of its initial volume. The resulting solution was mixed with a solution of phenylsalicylate (7.712 g, 36 mmol) and Et_3N (5 mL, 36 mmol) in propan-2-ol (90 mL). The reaction mixture was stirred at room temperature for 2 h and then warmed at about 60 °C for 12 h. Addition of a mixture of ethanol and water (1:10, 110 mL) yielded a white precipitate that was filtered off, washed with diethyl ether (20 mL) and dried. Yield: 1.3 g (40.3%). $C_{19}H_{22}N_2O_5$ (358.39): calcd. C 63.7, H 6.2, N 7.8; found C 63.7, H 6.3, N 7.8. IR (KBr pellet): $\tilde{\nu}$ = 3378, 3278 (ν_{OH} and ν_{NH}), 1646, 1636 ($\nu_{C=O}$), 1256 [ν_{CO}(phenoxido)], 1023 [ν_{CO}(alkoxido)] cm^{-1}. ^1H NMR (250 MHz, 20 °C, [D$_6$]DMSO): δ = 1.8 (m, 4 H, CHC*H*$_2$CH$_2$), 3.5 (m, 4 H, CHCH$_2$C*H*$_2$), 3.7 (m, 1 H, C*H*), 4.5 (s, 1 H, CHO*H*), 7.0 [m, 4 H, ArC(3)*H*, ArC(3′)*H*, ArC(5)*H*, ArC(5′)*H*], 7.5 [m, 2 H, ArC(4)*H*, ArC(4′)*H*], 7.9 [m, 2 H, ArC(6)*H*, ArC(6′)*H*], 8.9 (t, J = 5.3 Hz, 2 H, N*H*) ppm. ^{13}C NMR: δ = 36.5 (CH*C*H$_2$CH$_2$), 36.7 (CHCH$_2$*C*H$_2$), 66.2 (*C*H), 115.4 [Ar*C*-(3)H], 117.7 [Ar*C*(1)], 118.8 [Ar*C*(5)H], 127.7 [Ar*C*(6)H], 133.7 [Ar*C*(4)H], 160.3 [Ar*C*(2)OH], 169.1 (O*C*NH) ppm. UV/Vis: λ_{max} = 363 nm.

$[Cu_2(L^1)(OAc)Cs_2(MeOH)_2]_n$ (1): To a stirred solution of $CsOH\cdot H_2O$ (1.679 g, 10 mmol) in MeOH (5 mL) was added a suspension of H_5L^1 (0.661 g, 2 mmol) in MeOH (5 mL) and $Cu(OAc)_2\cdot H_2O$ (0.800 g, 4 mmol). The reaction mixture was stirred for 30 min at room temperature. The color of the solution immediately turned to blue. The solution was filtered and kept in a refrigerator for crystallization. After 3 d, blue crystals of **1** formed; they were filtered and washed with cold methanol. Yield 0.246 g (14.6%). Upon standing in air for a few hours, the crystals absorb water; the resulting samples analyze as $[Cu_2(L^1)(OAc)Cs_2(MeOH)_2]\cdot 2H_2O$. $C_{21}H_{28}Cs_2Cu_2N_2O_{11}$ (877.36): calcd. C 28.8, H 3.2, N 3.2; found C 28.8, H 3.1, N 3.3. IR (KBr pellet): $\tilde{\nu}$ = 3374 (ν_{OH}), 1597 ($\nu_{C=O}$), 1562 [ν_{COO}(asym)], 1460 [ν_{COO}(sym)], 1262 [ν_{CO}-(phenoxido)], 1044 [ν_{CO}(alkoxido)] cm^{-1}. TG analysis: 35–55 °C, weight loss 7.5% (calcd. for 2MeOH 7.3%), 55–220 °C weight loss 3.75% (calcd. for 2H_2O 4.1%). UV/Vis: (λ_{max} = 338, 377, 629 nm.

$[Mn_2(H_3L^1)_2(OMe)_2]\cdot 2MeOH$ (2): To a stirred solution of $Mn(ClO_4)_2\cdot 6H_2O$ (0.145 g, 0.4 mmol) in MeOH (10 mL) was added a solution of H_5L^1 (0.132 g, 0.4 mmol) in MeOH (10 mL) and a solution of NaOMe (0.043 g, 0.8 mmol) in MeOH (10 mL). The reaction mixture was stirred for 1 h at room temperature. The color of the solution immediately turned to dark brown. The solution was filtered and kept at room temperature for crystallization. After 3 d, dark reddish–brown crystals of **2** formed; they were filtered and washed with cold methanol. Yield 0.128 g (35.8%). Upon standing in air for a few hours, the crystals lose MeOH and absorb water. The resulting samples analyse as $[Mn_2(H_3L^1)_2(OMe)_2]\cdot 5H_2O$. $C_{36}H_{48}Mn_2N_4O_{17}$ (918.66): calcd. C 47.1, H 5.3, N 6.1; found C 46.9, H 4.9, N 6.0. IR (KBr pellet): $\tilde{\nu}$ = 3342 (ν_{OH}), 1611 ($\nu_{C=O}$), 1242 [ν_{CO}(phenoxido)], 1040 [ν_{CO}(alkoxido)] cm^{-1}. UV/Vis: λ_{max} = 347, 440, 549, 588, 658 nm.

$[Fe_2(H_3L^1)_2(Hpz)_4](ClO_4)_2\cdot 2CH_3CN$ (3): To a stirred solution of $Fe(ClO_4)_2\cdot 6H_2O$ (0.073 g, 0.2 mmol) in ethanol (1 mL) and acetonitrile (2 mL) was added a suspension of H_5L^1 (0.033 g, 0.1 mmol) in acetonitrile (2 mL), piperidine (0.02 mL, 0.2 mmol), and a solution of pyrazole (0.027 g, 0.4 mmol) in acetonitrile (1 mL). The re-

Table 1. X-ray crystallographic data for complexes **1**–**4**.

	1	**2**	**3**	**4**
Chemical formula	$C_{21}H_{24}Cs_2Cu_2N_2O_9$	$C_{38}H_{46}Mn_2N_4O_{14}$	$C_{50}H_{54}Cl_2Fe_2N_{14}O_{18}$	$C_{48}H_{78}Fe_2N_4O_{20}$
F_w	841.34	892.66	1321.67	1142.84
Space group	*Pnma*	$P2_1/c$	$P\bar{1}$	$P\bar{1}$
a [Å]	13.4687(6)	12.154(2)	10.683(5)	11.1253(7)
b [Å]	18.6557(7)	13.061(1)	11.041(5)	11.6251(3)
c [Å]	10.2024(4)	13.375(2)	12.820(5)	12.7793(8)
α [°]			92.751(5)	66.412(5)
β [°]		109.460(10)	94.454(5)	69.643(3)
γ [°]			93.292(5)	88.557(6)
V [Å^3]	2563.54(17)	2001.9(5)	1503.0(11)	1407.53(13)
Z	4	2	1	1
T [K]	180	180	180	180
λ [Å]	0.71073	0.71073	0.71073	0.71073
$\rho_{calcd.}$ [g cm^{-1}]	2.18	1.481	1.460	1.348
μ [mm^{-1}]	4.511	0.703	0.652	0.590
R_1[a]	0.0532[c]	0.0523[d]	0.0577[c]	0.063[c]
wR_2[b]	0.1295[c]	0.0575[d]	0.0971[c]	0.1812[c]
R_1 (all data)[a]	0.0619		0.1930	0.0698
wR_2 (all data)[b]	0.1356		0.1293	0.1901

[a] $R = \Sigma||F_o| - |F_c||/\Sigma|F_o|$. [b] $wR = [\Sigma w(|F_o^2| - |F_c^2|)^2/\Sigma w|F_o^2|^2]^{1/2}$. [c] $I > 2\sigma(1)$. [d] $I > 1.6\sigma(1)$.

action mixture was kept at room temperature. After 3 d, dark violet–reddish crystals of **3** formed; they were filtered and washed with cold acetonitrile. Yield 0.032 g (24.2%). $C_{50}H_{54}Cl_2Fe_2N_{14}O_{18}$ (1321.67): calcd. C 45.4, H 4.1, N 14.8; found C 44.8, H 3.7, N 14.5. IR (KBr pellet): $\tilde{\nu}$ = 3336 (ν_{OH}), 1605 ($\nu_{C=O}$), 1250 [ν_{CO}(phenoxido)], 1145, 1115, 1089 (ν_{ClO}), 1046 [ν_{CO}(alkoxido)] cm^{-1}. UV/Vis: λ_{max} = 359, 584 nm.

[$Fe_2(H_3L^3)_2(OMe)_2$]·8MeOH (4): To a stirred solution of $Fe(OAc)_2$ (0.044 g, 0.25 mmol) in MeOH (10 mL) was added a solution of H_5L^3 (0.045 g, 0.125 mmol) in MeOH (10 mL) and piperidine (0.06 mL, 0.625 mmol). The reaction mixture was stirred for 45 min at room temperature. The color of the solution immediately turned to orange. The solution was filtered and kept in a refrigerator for crystallization. After 3 d, orange crystals of **4** formed; they were filtered and washed with cold methanol. Yield 0.026 g (18.2%). Upon standing in air for a few minutes, the crystals lose MeOH and absorb water. The resulting samples analyse as [$Fe_2(H_3L^3)_2(OMe)_2$]·5H_2O. $C_{40}H_{56}Fe_2N_4O_{17}$ (976.59): calcd. C 49.2, H 5.8, N 5.7; found C 49.1, H 5.1, N 5.6. IR (KBr pellet): $\tilde{\nu}$ = 3317 (ν_{OH}), 1607 ($\nu_{C=O}$), 1256 [ν_{CO}(phenoxido)], 1028 [ν_{CO}(alkoxido)] cm^{-1}. UV/Vis: λ_{max} = 348, 505 nm.

Physical Measurements: Microanalyses for C, H and N were performed by the Microanalytical Laboratory of the Laboratoire de Chimie de Coordination at Toulouse. TG and DTA were carried out on a SETARAM 92–16.18 thermoanalyzer. Infrared spectra (4000–400 cm^{-1}) were recorded on a Perkin–Elmer Spectrum GX system 2000 FTIR spectrometer as KBr pellets. The electronic spectra (diffuse reflectance technique) were recorded with a UV4 UNICAM spectrophotometer in the range 280–820 nm with MgO as reference. Variable-temperature (1.8–300 K) magnetic susceptibility data were collected on freshly prepared crystalline samples of the complexes pressed into pellets (3-mm diameter) with a Quantum Design MPMS SQUID susceptometer under a 0.1 T applied magnetic field. Data were corrected with the standard procedure for the contribution of the sample holder and for diamagnetism of the samples.[69]

Crystallographic Data Collection and Structure Determination for 1, 2, 3, and 4: Crystals of **1**–**4** were kept in the mother liquor and then dipped into oil. Chosen crystals were mounted on a Mitegen micromount and quickly cooled down to 180 K. The selected crystal of **1** (blue, 0.25 × 0.15 × 0.05 mm) was mounted on an Oxford Diffraction XCALIBUR CCD diffractometer using a graphite-monochromated Mo-K_α radiation source (λ = 0.71073 Å) and equipped with an Oxford Cryosystems Cryostream Cooler Device. Selected crystals of **2** (dark reddish–brown, 0.30 × 0.30 × 0.06 mm) and **3** (dark violet–reddish, 0.20 × 0.10 × 0.05 mm) were mounted on a Stoe Imaging Plate Diffractometer System (IPDS) using a graphite monochromator (λ = 0.71073 Å) and equipped with an Oxford Cryosystems Cooler Device. The selected crystal of **4** (orange, 0.20 × 0.18 × 0.1 mm) was mounted on a Bruker Kappa APEX II diffractometer using a graphite-monochromated Mo-K_α radiation source (λ = 0.71073 Å) and equipped with an Oxford Cryosystems Cryostream Cooler Device. The data were collected at 180 K. Unit cell determination and data integration were carried out with the CrysAlis RED[70] (**1**), X*red*[71] (**2** and **3**), and Bruker[72] (**4**) packages. 22540 reflections were collected for **1**, of which 3521 were independent (R_{int} = 0.0994), 19871 reflections for **2**, of which 3814 were independent (R_{int} = 0.165), 15010 reflections for **3**, of which 5549 were independent (R_{int} = 0.1441), and 34549 reflections for **4**, of which 5193 were independent (R_{int} = 0.029). The structures of **1**–**3** were solved by using SIR 92[73] and that of **4** was solved by using SHELXS-86.[74] For complexes **1**, **3**, and **4**, the refinements were carried out by full-matrix least-squares on F^2 with SHELXL-97[75] included in the software package WinGX.[76] For complex **2**, the refinement was carried out by full-matrix least-squares on F with CRYSTALS.[77] For complex **1**, the O*H* hydrogen atom of the methanol molecule could not be located on atom O5. For complex **2**, all hydrogen atoms were located in difference maps, but those attached to carbon atoms were repositioned geometrically; the hydrogen atoms were initially refined with soft restraints on the bond lengths and angles to regularize their geometry. For complex **3**, the amide N*H* and pyrazole N*H* hydrogen atoms were first derived from Fourier difference maps but, as the refinements were unstable, they were finally fixed. The remaining hydrogen atoms were included in calculated positions and refined as riding atoms by using SHELX default parameters. All non-hydrogen atoms were refined with anisotropic displacement parameters. For complex **4**, the atoms C60 and O20 are statistically disordered over locations A and B with occupancy factors of 0.8 and 0.2. Absorption corrections were applied by using Multiscan[78] (**1**, **2**, and **4**) or DELABS/DIFABS[79] (**3**). The figures were drawn with ORTEP3[80] (**1**, **3**, **4**)

and Cameron (**2**).[81] Crystal data collection and refinement parameters are collated in Table 1. CCDC-743833 (**1**), -743834 (**2**), -743835 (**3**), and -743836 (**4**) contain the supplementary crystallographic data for this paper. These data can be obtained free of charge via www.ccdc.cam.ac.uk/data_request/cif.

Acknowledgments

Financial support by the Agence Universitaire de la Francophonie (AUF), through a postdoctoral grant "Bourse de Perfectionnement en Recherche" and by NATO through a "Reintegration Grant" (CBP.EAP.RIG.982417) to L. S. is gratefully acknowledged.

[1] J.-P. Costes, S. Shova, W. Wernsdorfer, *Dalton Trans.* **2008**, 1843–1849 and references cited therein.
[2] T. Hamamatsu, K. Yabe, M. Towatari, N. Matsumoto, N. Re, A. Pochaba, J. Mrozinski, *Bull. Chem. Soc. Jpn.* **2007**, *80*, 523–529.
[3] R. Tao, F. Li, S. Zang, Y. Cheng, J. Niu, *Sci. China, Ser. B* **2006**, *49*, 338–344.
[4] R.-J. Tao, F.-A. Li, S.-Q. Zang, Y.-X. Cheng, Q.-L. Wang, J.-Y. Niu, D.-Z. Liao, *Polyhedron* **2006**, *25*, 2153–2159.
[5] J.-P. Costes, J. M. Clemente-Juan, F. Dahan, J. Milon, *Inorg. Chem.* **2004**, *43*, 8200–8202.
[6] S. Osa, T. Kido, N. Matsumoto, N. Re, A. Pochaba, J. Mrozinski, *J. Am. Chem. Soc.* **2004**, *126*, 420–421 and references cited therein.
[7] S. Osa, Y. Sunatsuki, Y. Yamamoto, M. Nakamura, T. Shimamoto, N. Matsumoto, N. Re, *Inorg. Chem.* **2003**, *42*, 5507–5512.
[8] T. C. Harrop, M. M. Olmstead, P. K. Mascharak, *Chem. Commun.* **2003**, 410–411.
[9] M. Papadopoulos, B. Nock, T. Maina, I. Pirmettis, C. Raptopoulou, A. Tasiopoulos, A. Troganis, T. Kabanos, A. Terzis, E. Chiotellis, *J. Biol. Inorg. Chem.* **2001**, *6*, 159–165.
[10] M. Koikawa, H. Okawa, N. Matsumoto, M. Gotoh, S. Kida, T. Kohsuma, *J. Chem. Soc., Dalton Trans.* **1989**, 2089–2094 and references cited therein.
[11] S. Louhibi, A. Y. Nour, L. Vendier, J.-P. Costes, J.-P. Tuchagues, *Polyhedron* **2007**, *26*, 3448–3454.
[12] P. K. Nanda, D. Ray, *J. Chem. Res.* **2006**, 632–635.
[13] M. R. Maurya, J. J. Titinchi, S. Chand, *Catal. Lett.* **2003**, *89*, 219–227.
[14] C. A. Sureshan, P. K. Bhattacharya, *Indian J. Chem. Sect. A: Inorg. Bio-Inorg. Phys. Theor. Anal. Chem.* **1999**, *38A*, 723–726.
[15] Y. Sunatsuki, T. Matsuo, M. Nakamura, F. Kai, N. Matsumoto, J.-P. Tuchagues, *Bull. Chem. Soc. Jpn.* **1998**, *71*, 2611–2619 and references cited therein.
[16] Y. Sunatsuki, M. Nakamura, N. Matsumoto, F. Kai, *Bull. Chem. Soc. Jpn.* **1997**, *70*, 1851–1858.
[17] O. Rotthaus, O. Jarjayes, F. Thomas, C. Philouze, C. P. Del Valle, E. Saint-Aman, J.-L. Pierre, *Chem. Eur. J.* **2006**, *12*, 2293–2302.
[18] S. Mukerjee, K. Skogerson, S. DeGala, J. P. Caradonna, *Inorg. Chim. Acta* **2000**, *297*, 313–329.
[19] S. Nayak, A. C. Dash, G. K. Lahiri, *Transition Met. Chem.* **2008**, *33*, 39–53.
[20] C. A. Jimenez, J. B. Belmar, J. Alderete, F. S. Delgado, M. Lopez-Rodriguez, O. Pena, M. Julve, C. Ruiz-Perez, *Dalton Trans.* **2007**, 2135–2144.
[21] Y. Sunatsuki, M. Mimura, H. Shimada, F. Kai, N. Matsumoto, *Bull. Chem. Soc. Jpn.* **1998**, *71*, 167–173.
[22] F. C. Anson, T. J. Collins, R. J. Coots, S. L. Gipson, T. G. Richmond, *J. Am. Chem. Soc.* **1984**, *106*, 5037–5038.
[23] G. T. Rowe, E. V. Rybak-Akimova, J. P. Caradonna, *Inorg. Chem.* **2007**, *46*, 10594–10606.
[24] T. L. Foster, J. P. Caradonna, *J. Am. Chem. Soc.* **2003**, *125*, 3678–3679.
[25] P. J. Cappillino, P. C. Tarves, G. T. Rowe, A. J. Lewis, M. Harvey, C. Rogge, A. Stassinopoulos, W. Lo, W. H. Armstrong, J. P. Caradonna, *Inorg. Chim. Acta* **2009**, *362*, 2136–2150 and references cited therein.
[26] M. R. Maurya, S. J. J. Titinchi, S. Chand, *J. Mol. Catal. A* **2004**, *214*, 257–264.
[27] P. K. S. Chowdhury, U. Mukhopadhyay, D. Ray, *Indian J. Chem. Sect. A: Inorg. Bio-Inorg. Phys. Theor. Anal. Chem.* **1999**, *38A*, 1159–1163.
[28] Z. Smekal, Z. Sindelar, R. Klicka, *Monatsh. Chem.* **1998**, *129*, 769–776.
[29] K. Bertoncello, G. D. Fallon, K. S. Murray, *Inorg. Chim. Acta* **1990**, *174*, 57–60.
[30] L. Stoicescu, A. Jeanson, C. Duhayon, A. Tesouro-Vallina, A. K. Boudalis, J.-P. Costes, J.-P. Tuchagues, *Inorg. Chem.* **2007**, *46*, 6902–6910.
[31] Y. Sunatsuki, H. Shimada, T. Matsuo, M. Nakamura, F. Kai, N. Matsumoto, N. Re, *Inorg. Chem.* **1998**, *37*, 5566–5574.
[32] K. Bertoncello, G. D. Fallon, K. S. Murray, *Polyhedron* **1990**, *9*, 2867–2871.
[33] S. K. Chandra, A. Chakravorty, *Inorg. Chem.* **1992**, *31*, 760–765 and references cited therein.
[34] T. J. Collins, B. D. Santarsiero, G. H. Spies, *J. Chem. Soc., Chem. Commun.* **1983**, 681–682.
[35] T. Ma, T. Kojima, Y. Matsuda, *Polyhedron* **2000**, *19*, 1167–1172.
[36] A. D. Keramidas, A. B. Papaioannou, A. Vlahos, T. A. Kabanos, G. Bonas, A. Makriyannis, C. P. Rapropoulou, A. Terzis, *Inorg. Chem.* **1996**, *35*, 357–367 and references cited therein.
[37] C. M. Che, W. K. Cheng, W. H. Leung, T. C. W. Mak, *J. Chem. Soc., Chem. Commun.* **1987**, 418–419.
[38] K.-L. Yip, W.-Y. Yu, P.-M. Chan, N.-Y. Zhu, C.-M. Che, *Dalton Trans.* **2003**, 3556–3566 and references cited therein.
[39] T. J. Collins, T. Lai, G. T. Peake, *Inorg. Chem.* **1987**, *26*, 1674–1677.
[40] T. J. Collins, J. T. Keech, *J. Am. Chem. Soc.* **1988**, *110*, 1162–1167 and references cited therein.
[41] F. C. Anson, T. J. Collins, S. L. Gipson, T. E. Krafft, *Inorg. Chem.* **1987**, *26*, 731–736 and references cited therein.
[42] L. Luo, W. P.-W. Lai, K.-L. Wong, W.-T. Wong, K.-F. Li, K.-W. Cheah, *Chem. Phys. Lett.* **2004**, *398*, 372–376.
[43] B. Zhoa, W. Yang, J. Gao, Z. Mo, X. Zhang, Q. Deng, J. Hou, *Rare Met. (Beijing, China)* **1999**, *18*, 209–216.
[44] W. Yang, Q.-Y. Ou, W. Yang, Z.-L. Mo, X.-L. Teng, M. Chen, J.-Z. Gao, L. Yuan, J.-W. Kang, *Analyst (Cambridge, U. K.)* **1998**, *123*, 1745–1748.
[45] S. M. Cohen, M. Meyer, K. N. Raymond, *J. Am. Chem. Soc.* **1998**, *120*, 6277–6286.
[46] R. Shukla, P. K. Bharadwaj, U. C. Johri, *Polyhedron* **1993**, *12*, 1553–1557.
[47] J.-P. Costes, F. Dahan, B. Donnadieu, M.-J. Rodriguez Douton, M.-I. Fernandez Garcia, A. Bousseksou, J.-P. Tuchagues, *Inorg. Chem.* **2004**, *43*, 2736–2744.
[48] W. Mazurek, B. J. Kennedy, K. S. Murray, M. J. O'Connor, J. R. Rodgers, M. R. Snow, A. G. Wedd, P. Zwack, *Inorg. Chem.* **1985**, *24*, 3258–3264.
[49] Y. Nishida, S. Kida, *J. Chem. Soc., Dalton Trans.* **1986**, 2633–2640.
[50] V. A. Kogan, V. V. Lukov, V. M. Novotortsev, I. L. Eremenko, G. G. Aleksandrov, *Russ. Chem. Bull.* **2005**, *54*, 600–605.
[51] W. J. Evans, J. H. Hain Jr., R. N. R. Broomhall-Dillard, J. W. Ziller, *J. Coord. Chem.* **1999**, *47*, 199–209.
[52] D. Guo, B. G. Zhang, C. Y. Duan, K. L. Pang, Q. J. Meng, *J. Chem. Soc., Dalton Trans.* **2002**, 3783–3784.
[53] H. G. Visser, *Acta Crystallogr., Sect. E* **2007**, *63*, m162–m164.
[54] M. Tadokoro, T. Shiomi, K. Isobe, K. Nakasuji, *Inorg. Chem.* **2001**, *40*, 5476–5478.
[55] X. S. Tan, W. X. Tang, *Polyhedron* **1996**, *15*, 2671–2675.

[56] T. K. Paine, T. Weyhermüller, E. Bothe, K. Wieghardt, P. Chaudhuri, *Dalton Trans.* **2003**, 3136–3144 and references cited therein.
[57] C. Beghidja, G. Rogez, J. Kortus, M. Wesolek, R. Welter, *J. Am. Chem. Soc.* **2006**, *128*, 3140–3141.
[58] S. Negoro, H. Asada, M. Fujiwara, T. Matsushita, *Inorg. Chem. Commun.* **2003**, *6*, 357–360.
[59] H. Houjou, M. Kanesato, K. Hiratani, D. Mandon, *Chem. Eur. J.* **2004**, *10*, 4576–4583.
[60] S. J. Barclay, P. E. Riley, K. N. Raymond, *J. Am. Chem. Soc.* **1982**, *104*, 6802–6804.
[61] a) B. Chiari, O. Piovesana, T. Tarantelli, P. F. Zanazzi, *Inorg. Chem.* **1982**, *21*, 1396–1402; b) B. Chiari, O. Piovesana, T. Tarantelli, P. F. Zanazzi, *Inorg. Chem.* **1984**, *23*, 3398–3404.
[62] R. Viswanathan, M. Palaniandavar, P. Prabakaran, P. T. Muthiah, *Inorg. Chem.* **1998**, *37*, 3881–3884.
[63] C. J. O'Connor, *Prog. Inorg. Chem.* **1982**, *29*, 203–283.
[64] P. Garge, R. Chikate, S. Padhye, J. M. Savariault, P. De Loth, J.-P. Tuchagues, *Inorg. Chem.* **1990**, *29*, 3315–3320 and references therein.
[65] A. P. Ginsberg, M. E. Lines, *Inorg. Chem.* **1972**, *11*, 2289–2290.
[66] R. Boča, *Coord. Chem. Rev.* **2004**, *248*, 757–815.
[67] C.-H. S. Wu, G. R. Rossman, H. B. Gray, G. S. Hammond, H. J. Schugar, *Inorg. Chem.* **1972**, *11*, 990–994.
[68] I. Murase, M. Hatano, M. Tanaka, S. Ueno, H. Okawa, S. Kida, *Bull. Chem. Soc. Jpn.* **1982**, *55*, 2404–2408.
[69] P. Pascal, *Ann. Chim. Phys.* **1910**, *19*, 5–70.
[70] CrysAlis RED Oxford Diffraction Ltd.,Version 1.171.32, **2007**.
[71] *STOE: IPDS Manual*, version 2.75, Stoe & Cie, Darmstadt, Germany, **1996**.
[72] *Bruker APEX2 and SAINT*, Bruker AXS Inc, Madison, Wisconsin, USA, **2004**.
[73] A. Altomare, G. Cascarano, C. Giacovazzo, A. Guagliardi, M. C. Burla, G. Polidori, M. Camalli, *J. Appl. Crystallogr.* **1994**, *27*, 435–436.
[74] G. M. Sheldrick, *SHELXS86: Program for the Solution of Crystal Structures*, Institüt für Anorganische Chemie der Universität, Göttingen, Germany, **1986**.
[75] G. M. Sheldrick, *SHELXL-97, Program for the Refinement of Crystal Structures*, University of Göttingen, Germany, **1997**.
[76] L. J. Farrugia, *J. Appl. Crystallogr.* **1999**, *32*, 837–838.
[77] P. W. Betteridge, J. R. Carruthers, R. I. Cooper, K. Prout, D. J. Watkin, *J. Appl. Crystallogr.* **2003**, *36*, 1487.
[78] R. H. Blessing, *Acta Crystallogr., Sect. A* **1995**, *51*, 33–38.
[79] N. Walker, D. Stuart, *Acta Crystallogr., Sect. A* **1983**, *39*, 158–166.
[80] ORTEP3 for Windows: L. J. Farrugia, *J. Appl. Crystallogr.* **1997**, *30*, 565.
[81] D. J. Watkin, C. K. Prout, L. J. Pearce, *CAMERON*, Chemical Crystallography Laboratory, University of Oxford, Oxford, UK, **1996**.

Received: August 13, 2009
Published Online: November 5, 2009

